Electronic Supplementary Material (ESI) for Nanoscale.
This journal is © The Royal Society of Chemistry 2022

GaAs/GaP superlattice nanowires: growth, vibrational and optical properties

Omer Arif,[a] Valentina Zannier,[a] Francesca Rossi,[b] Diego De Matteis,[c] Katharina Kress,[c] Marta De Luca,[c,d] Ilaria Zardo,[c] and Lucia Sorba,[*a]

a. NEST, Istituto Nanoscienze—CNR and Scuola Normale Superiore, Piazza San Silvestro 12, I-56127 Pisa, Italy
b. IMEM—CNR, Parco Area delle Scienze 37/A, I-43124 Parma, Italy
c. Physics Department, University of Basel, Klingelbergstrasse 82, CH-4056 Basel, Switzerland
d. Physics Department, Sapienza University of Rome, P.le Aldo Moro 2, 00185 Rome, Italy

Electronic supplementary information

S1. Growth optimization

As a first step for optimizing the growth conditions for the GaAs/GaP SL NWs, we investigated the effect of the Au film thickness on the distribution of the length of GaAs stem and GaP segment grown for 30 minutes as a function of the nanoparticle diameter. Figure S1a and b show SEM images of GaAs/GaP NWs (growth interrupted after step II) obtained with 0.1 nm and 0.5 nm thick Au film, respectively. The presence of gold droplets on the top of each NW confirms the growth through vapor liquid solid (VLS) mechanism. The GaAs/GaP NWs obtained from 0.1 nm thick Au film are quite uniform in diameter and length as seen in panel (a), while in the case of 0.5 nm thick Au film the NWs have different diameters and inhomogeneous length distribution (panel b).

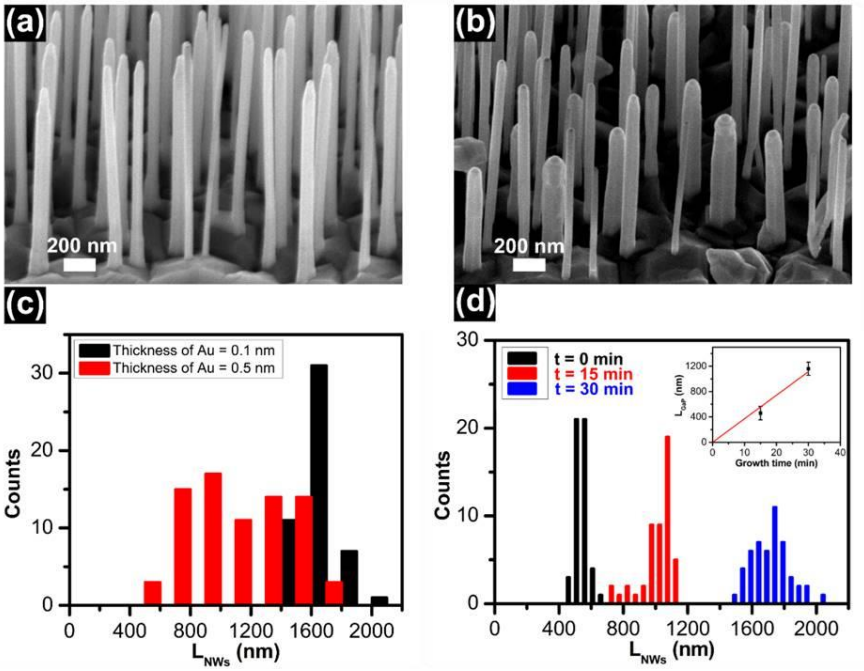

Figure S 1 (a)-(b) 45° tilted SEM images of GaAs/GaP NWs (growth stopped after step II) corresponding to 0.1 nm and 0.5 thick Au film, respectively. (c) Length distributions of GaAs/GaP NWs for the two different Au film thicknesses. (d) Time evolution of length distribution of the GaAs/GaP NWs obtained using 0.1 nm thick Au film. Time t = 0 min corresponds to the length distribution of the GaAs stems. The inset shows the length of the GaP (L_{GaP}) segments as a function of growth time. The growth rate is extracted from the linear fit of L_{GaP} vs growth time.

In particular, there are long and thin NWs similar to the NWs obtained with 0.1 nm Au, but also shorter and thicker NWs. In order to quantify the difference of the two samples, SEM images were taken from several different regions and the lengths of NWs and diameters of Au nanoparticles were measured. The length distributions of the two samples are shown in panel (c) of (Fig. S1), while the length versus diameter dispersion is shown in (Fig. 1a) of the main text. For 0.1 nm Au film thickness, the average values of length of NWs and diameter of Au nanoparticles are 1710 ± 95 nm and 42 ± 5 nm, respectively. In the case of 0.5 nm thick Au film,

 This journal is © The Royal Society of Chemistry 20xx

both length and diameter distribution are instead much broader. In fact, there the average length of NWs and diameter of Au nanoparticles are 1085 ± 313 nm and 55 ± 13 nm, respectively.

Since 0.1 nm thick Au film provides a narrower length and diameter distribution than 0.5 nm thick Au film, we decided to use 0.1 nm thick Au film for the growth of GaAs/GaP SL NWs. Before growing the SL segment, we investigated the growth rate of the GaP segment. In Fig. S1d the histogram at time t = 0 min represents the length distribution of GaAs stems (L_{GaAs}). Then, we grew the GaP segments for different times (15 and 30 min) on top of these GaAs stems. We found that the length distribution for GaAs stems is very narrow, while for GaP segments is larger and it broadens with increasing the growth time. The inset in (Fig. S1d) shows the average length of the GaP (L_{GaP}) segment, calculated as $L_{NWs} - L_{GaAs}$, as a function of growth time. The axial growth rate derived from the slope of the linear fit of the experimental data points is 37 ± 3 nm/min.

S2. STEM analysis of the GaAs/GaP SL sample

Figure S2 shows the STEM image of a representative GaAs/GaP SL NW without GaP top segment (growth terminated after step III), with the SL segment made of 100 repetition of 3 nm GaAs and 3 nm GaP (nominal thickness), similar to the SL segment of the NWs analyzed by Raman and μ–PL (reported in the main text). The STEM analysis confirmed the formation of GaAs layers of 3.2 ± 0.4 nm average thickness and GaP layers of 3.8 ± 0.5 nm average thickness.

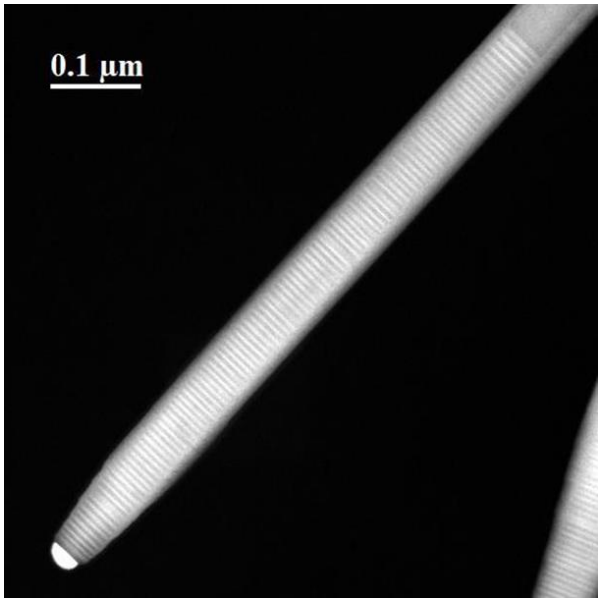

Figure S 2 STEM image of the upper portion of a GaAs/GaP SL NWs without the GaP top segment, where the 100 repetitions of 3 nm GaAs and 3 nm GaP alternating segments is visible thanks to the Z contrast.

S3. Raman spectra of reference NWs without SL segments

We performed μ-Raman measurements on single GaAs/GaP NWs (without SL), like the ones shown in (Figure S1a). This allowed us to single out the effect of the SL on the Raman spectrum. We display in Figure S3 a spectrum taken from such a NW, together with the scanning electron micrograph of the measured wire. The spectrum displays typical and expected features of WZ phase GaAs and GaP: the GaAs TO mode at ~266 cm^{-1}; a low intensity feature at ~350 cm^{-1} the GaP $\boldsymbol{E_2^H}$ mode; the GaP TO mode at ~ 363 cm^{-1}; a GaP Surface Optical (SO) mode at ~385 cm^{-1}; the GaP LO mode at ~399 cm^{-1}. These measurements confirm that we can expect to see a small contribution from the GaAs NW stem (grown during step I). Noteworthy, the GaAs TO mode is at ~266 cm^{-1} similar to bulk GaAs at variance with the GaAs-like signal measured in the bottom part of the GaAs/GaP/SL/GaP NWs further confirming the different origin of these signals, as stated in the main text. While the observation of SO modes has been reported to be typical of NWs, and in particular of GaP NWs,[1] the observation of the GaP $\boldsymbol{E_2^H}$ mode and LO modes do not follow the selection rules expected for the scattering geometry, but it is readily understandable considering some experimental details. Namely, we employ a high NA objective, which means scattered photons with wave vectors not perpendicular to the NW surface are also collected. Furthermore, due to the hexagonal cross section of the NWs, we illuminate facets that are not perpendicular to the incident photons.[2] These photons with wavevector not perpendicular to the [2-1-10] facets of the NWs result in weak contributions

 This journal is © The Royal Society of Chemistry 20xx

from otherwise forbidden modes like in this case the GaP E_2^H and LO phonons. It is also important to note that the observation of the E_2^H mode in this scattering configuration, although forbidden, is a confirmation of the WZ phase GaP.

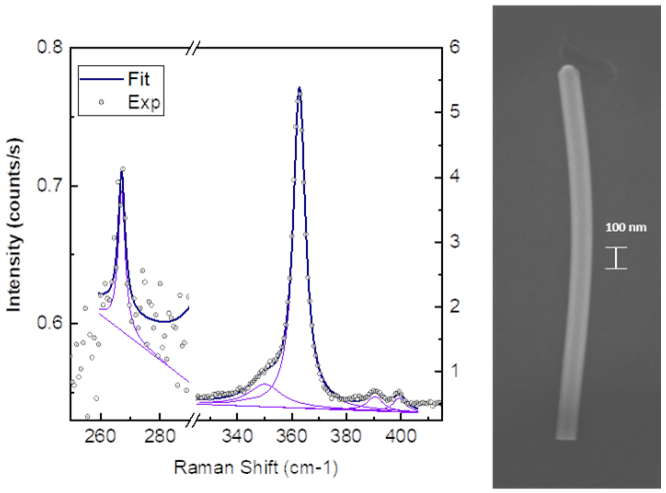

Figure S 3 Raman spectrum (left) from a reference NW (right: SEM image of the measured NW). The experimental data (empty symbols) are shown together with the Lorentzian curves used in the fit (solid lines).

S4. Photoluminescence spectra of reference NWs without SL segments

In order to confirm the interpretation of the newly observed band at ~1.66 eV in our SL NWs, we also measured reference GaAs/GaP NWs without SL segment, namely NWs singled out from the ensemble shown in (Fig. S1a). Figure S4 shows the comparison between μ-PL spectra of a SL NWs (panel (a)) different than the one in Fig. 5 in the main text, and the μ-PL spectra of reference NWs (panel (b)). At the NW center (top spectra, indicated by a red triangle as in the main text), only the SL NWs exhibit the SL band at 1.65 eV, which confirms the attribution discussed in the main text. In the SL NWs we also detect emission related to the pure GaAs-related and GaP-related bands in the SL (see dashed lines in panel (a)).

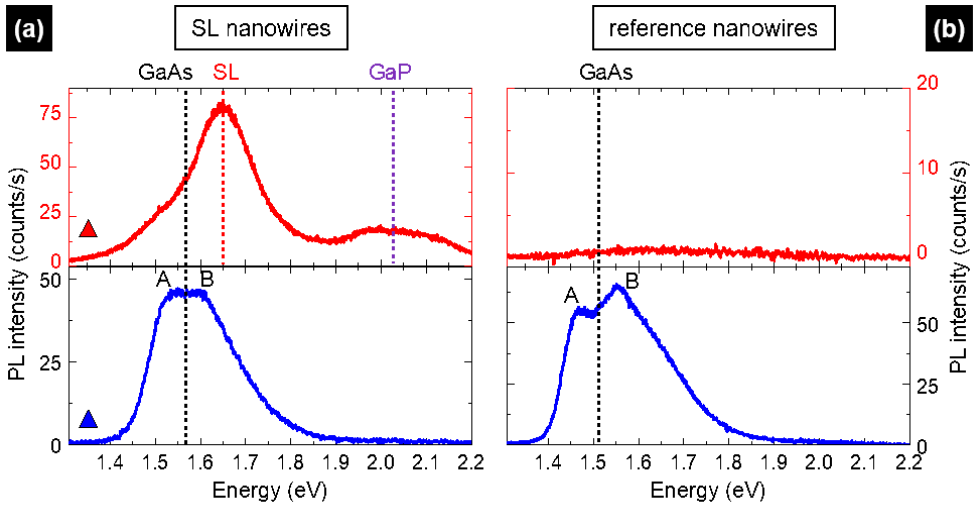

Figure S 4 Room-temperature μ-PL spectra of: (a) NWs containing a GaAs/GaP SL (similar to those discussed in Figure 5 in the main text); (b) reference NWs without SL. The bottom spectra (blue lines) were collected on the bottom GaAs/GaP stem, the top spectra (red lines) were collected approximately in the central-upper region of the NWs, where the SL is expected in the SL NWs. In both panels, dotted lines mark as a guide to the eye the average energy of transition A and B of the GaAs band observed at the bottom of the NWs. We point out that the NWs in panel (a) and (b) are both no single but double NWs. We noticed that the GaAs-related band is more likely to be observed in double NWs or NW bundles, likely because they have a lower probability to be broken during NW manipulation.

At the NW base (bottom spectra, blue triangles), both types of NWs exhibit GaAs-related bands in correspondence of the GaAs stem. The GaAs band, centered at ~1.57 eV in (Fig. S4a), is composed of two contributions, at ~1.53 and ~1.60 eV, the low energy

one being related to transition A (heavy holes) in WZ GaAs and the high energy one to transition B (light holes).[3,4] The high intensity of the B band is due to a hot carrier effect previously observed in InP and GaAs NWs at room temperature.[5]
Several points (either 1 in the center or 3 to 10 distributed along the NWs) were measured along several NWs (7 reference NWs and 4 SL NWs), the reference NWs all showing absence of SL band while the SL NWs all showing a localized SL band at ~1.65-1.66 eV. The GaAs band associated to the GaAs stem, instead, displayed some wire-to-wire variations in energy and relative intensity of the two peaks in both the reference and the SL NWs, as also visible by comparing the blue spectra in (Fig. S4a and b). Finally, in all the NWs (both reference and SL ones), the energy of the A and B GaAs bands was ~30 to ~110 meV larger than the one expected for WZ GaAs having these quite big base diameters (90 ± 15 nm).[6] This blueshift can be due to the strain typically introduced in the GaAs/GaP growth.[4]

S5. Raman and PL spectra under excitation of light with polarization perpendicular to the nanowire growth axis

We performed μ-Raman and μ-PL measurements on single nanowires with a 6 nm period GaAs/GaP SL also under excitation and detection of light with polarization perpendicular to the nanowire growth axis. We display in Figure S5 the Raman spectra taken under such polarization configuration (YY). Because of the dielectric mismatch effect, the Raman scattering intensity is considerably lower than in parallel polarization configuration (ZZ). The signal is often weak enough to be barely above the background and as such its fitting is unreliable and does not provide valuable information. The only use of perpendicular polarization spectra we found is to confirm the assignation of the E_2^H mode, indicating the hexagonal symmetry of the lattice. Interestingly, the scattering intensity under perpendicular scattering configuration is higher on the SL in comparison with the signal collected from regions outside of the SL, further indicating that the SL behaves as a different "material" and, therefore, the different phonon modes do not necessarily have the same scattering cross section as the one of the two individual materials forming the SL.

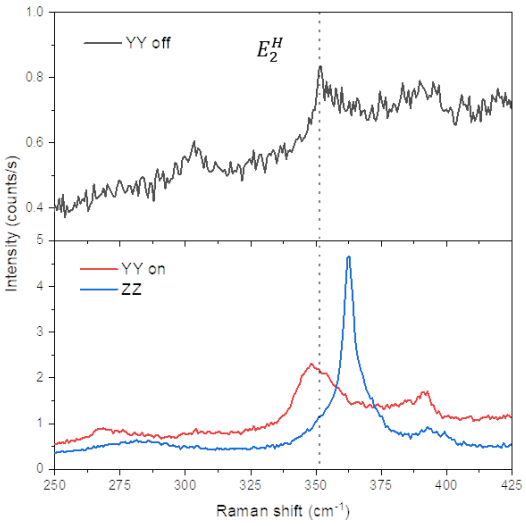

Figure S 5 Raman spectra collected with laser polarization and light detection vectors both perpendicular (YY) or both parallel (ZZ) to the NW long symmetry axis (aligned with the Z axis of the reference system) on the SL region (bottom panel) and outside it (top panel).

We display in Figure S6 the PL spectra taken under the same two polarization configurations as the Raman spectra (YY, red line, and ZZ, blue line) on the SL region of a NW singled out from the same batch (6 nm period). The SL band in YY is slightly more intense than in ZZ, with a degree of linear polarization of ~10%. The PL degree of polarization depends on the interplay between the electronic selection rules (that in WZ NWs favor the YY polarization)[3] and the optical dielectric mismatch effect (that tends to favor the ZZ polarization[3], as explained above). Our result suggests that the electronic selection rules are the dominant contribution to the degree of polarization.

This journal is © The Royal Society of Chemistry 20xx

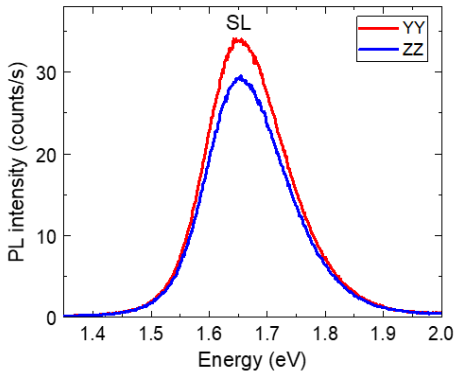

Figure S 6 PL spectra collected with laser polarization and light detection vectors both perpendicular (YY) or both parallel (ZZ) to the NW long symmetry axis on the SL region. The signal outside it is very low, as discussed in the main text.

References

1 R. Gupta, Q. Xiong, G. D. Mahan and P. C. Eklund, *Nano Lett*, 2003, **3**, 1745-1750.
2 C. Fasolato, I. Zardo and M. De Luca, in *Fundamental Properties of Semiconductor Nanowires*, eds. N. Fukata and R. Rurali, Springer Singapore, Singapore, 2021, DOI: 10.1007/978-981-15-9050-4_7, pp. 307-348.
3 M. De Luca, G. Lavenuta, A. Polimeni, S. Rubini, V. Grillo, F. Mura, A. Miriametro, M. Capizzi and F. Martelli, *Physical Review B*, 2013, **87**, 1-8.
4 G. Signorello, E. Lortscher, P. A. Khomyakov, S. Karg, D. L. Dheeraj, B. Gotsmann, H. Weman and H. Riel, *Nat Commun*, 2014, **5**, 3655.
5 D. Tedeschi, M. De Luca, H. A. Fonseka, Q. Gao, F. Mura, H. H. Tan, S. Rubini, F. Martelli, C. Jagadish, M. Capizzi and A. Polimeni, *Nano Lett*, 2016, **16**, 3085-3093.
6 B. Loitsch, D. Rudolph, S. Morkotter, M. Doblinger, G. Grimaldi, L. Hanschke, S. Matich, E. Parzinger, U. Wurstbauer, G. Abstreiter, J. J. Finley and G. Koblmuller, *Adv Mater*, 2015, **27**, 2195-2202.